NUCLEAR ORIENTATION OF ^{156}Tb IN GADOLINIUM MATRIX

J. Říkovská*), A. Machová**)

Czech Technical University, Prague

W. D. Hamilton

University of Sussex, Brighton, UK

J. Dupák, Chan Chen Mo, M. Finger, N. A. Lebedev, B. S. Neganov, V. N. Pavlov
A. F. Shchus

Joint Institute for Nuclear Research, Dubna, USSR

The anisotropy of the angular distribution of gamma-rays from the decay of ^{156}Tb, oriented in a gadolinium matrix at low temperatures, has been measured at the angles of 0 and $\pi/2$ with respect to the applied magnetic field direction in the range of temperatures from 14·6 to 68·4 mK. The temperature dependence of anisotropy was measured for the first time. The parameters of hyperfine magnetic dipole and electric quadrupole splittings have been determined and the values of the magnetic dipole moment $|\mu^{156}| = (9{\cdot}6 \pm 1{\cdot}3) \times 10^{-27}$ J/T and the electric quadrupole moment $Q^{156} = (2{\cdot}9 \pm 0{\cdot}9) \times 10^{-28}$ m^2 of the ^{156}Tb ground state have been calculated. Multipole mixing ratios and $B(E2)$ branching ratios of many gamma-ray transitions occurring in ^{156}Gd have been found and the results have been discussed in terms of the rotational-vibration and pairing-plus-quadrupole models.

1. INTRODUCTION

Nuclear orientation of ^{156}Tb was measured firstly by Lovejoy and Shirley [1]. The ^{156}Tb nuclei were oriented in a crystal of neodymium ethylsulfate cooled to low temperatures by adiabatic demagnetization. Anisotropies of several gamma-rays in ^{156}Gd were studied as a function of temperature, external magnetic field and magnetic environment. The spin of the ^{156}Tb ground state was shown to be 3 with $|\mu^{156}| = (7.32 \pm 0{\cdot}91) \times 10^{-27}$ J/T (1 J/T = 1·979825 $\times$ 10^{26} nuclear magnetons) and $Q^{156} = (1{\cdot}4 \pm 0{\cdot}5) \times 10^{-28}$ m^2. Using gamma-gamma and e_K-gamma direction correlation and nuclear orientation techniques, Uluer et al. [2] have determined the multipole character of many gamma-ray transitions in ^{156}Gd. The nuclear orientation measurements were carried out at low temperatures obtained with a ^{3}He + ^{4}He dilution refrigerator. Samples were prepared by implanting radioactive ^{156}Tb atoms into a gadolinium ferromagnetic matrix.

*) *Faculty of Mechanical Engineering, Department of Physics, Suchbatarova 4, Prague 6, Czechoslovakia.*

**) *Faculty of Nuclear Physics and Technical Engineering, Křemencova 10, Prague 1, Czechoslovakia.*

Parameters of the hyperfine interaction of ^{156}Tb nuclei dissolved in gadolinium have not been measured yet. The present work was undertaken in an attempt to determine these parameters and to obtain new information about magnetic dipole and electric quadrupole moments of ^{156}Tb. New data about mixing ratios and $B(E2)$ branching ratios for some gamma-ray transitions in ^{156}Gd were obtained and compared with recent theoretical results of GUPTA, KUMAR and HAMILTON [3].

2. EXPERIMENTAL PROCEDURE

The ^{156}Tb ($T_{1/2}$ = 5·4 d) activity was produced at the cyclotron of INR Kiyev, USSR. A gadolinium target was bombarded with 13 MeV deuterons and terbium activity was obtained using the standard ion exchange method [4]. Samples for the nuclear orientation experiments were prepared by implanting radioactive ^{156}Tb atoms into a gadolinium matrix (purity 99·9%). The implantation was performed on the electromagnetic mass-separator at a potential of 25 kV. The gadolinium matrix had been prepared by melting ~0·05 g of gadolinium onto a tantalum foil (thickness ~0·1 mm) in a vacuum furnace. After implantation a sample was melted again for a few seconds. Then a controlled cooling followed to the temperature of about 950 °C, further the cooling was free. The whole heat treatment was performed in vacuum of about 10^{-4} Pa.

The tantalum foil with the ^{156}Tb(Gd) sample was then soldered in vacuum at the temperature of about 800 °C onto a copper backing of the thickness of 0·5 mm, using an alloy of CuAgTi as a solder. The surface of the sample was grinded and cleaned and then the sample was formed to a flat rotation ellipsoid shape. Concentration of ^{156}Tb atoms in such a sample was less than 0·1%.

The sample preparation technology described above enables us to obtain a homogeneous structure of the Tb – Gd solid solution without internal stresses and to gain a good thermal contact with a cooling equipment.

The sample was cooled to the temperature of 14 mK by a contact with the cold-finger of a ^{3}He + ^{4}He dilution refrigerator [5]. The temperature was determined using a thermometer of ^{54}Mn in Ni [6], soldered to the cold-finger along with the Tb sample. The ferromagnetic Gd and Ni matrices were forced to the state of magnetic saturation by an external magnetic field of 0·85 T provided by a pair of superconducting coils. For ^{54}Mn(Ni) and ^{156}Tb(Gd) samples the demagnetizing fields DM (see Sec. 4.1) [7] were 0·028 T and 0·15 T respectively.

Gamma-rays were measured at the angles of 0 and $\pi/2$ with respect to the applied external magnetic field using two Ge(Li) coaxial detectors with a sensitive volume of about 30 cc and a resolution of 3 keV at 1332 keV both. The pulses from the detectors were registered by two 4096-channel analysers ICA-70. The energy spectrum was read onto a magnetic tape unit of the computer MINSK-2. The gamma-ray spectra were analysed on the ICL4-72 computer by the standard nonlinear least

squares method. The full-energy peaks were approximated by a symmetrical Gaussian line combined with a linear background.

For both mentioned angles the temperature dependence of gamma-ray intensities was measured at 15 points in the range of temperatures from 14·6 to 68·4 mK ("cold" spectra) and at the point of about 500 mK ("warm" spectrum).

3. EXPERIMENTAL RESULTS

Fig. 1 shows a typical gamma-ray "warm" spectrum of the ^{156}Tb source, taken with the 30cc Ge(Li) detector at the angle of 0 with respect to the applied external magnetic field. Normalized intensities $W^{exp}(\vartheta, T) = I^{\gamma}_{T=14.6mK}(\vartheta)/I^{\gamma}_{T\geq 500mK}(\vartheta)$ of 20 gamma-ray transitions are listed in Tab. 1. The values for the 1266·6 and 1815·0 keV transitions were measured for the first time. Experimental errors of W^{exp} were determined following the method used in [12]. Corresponding values for the temperature $T = 10{\cdot}4(2)$ mK, given by ULUER et al., [2], are presented for comparison.

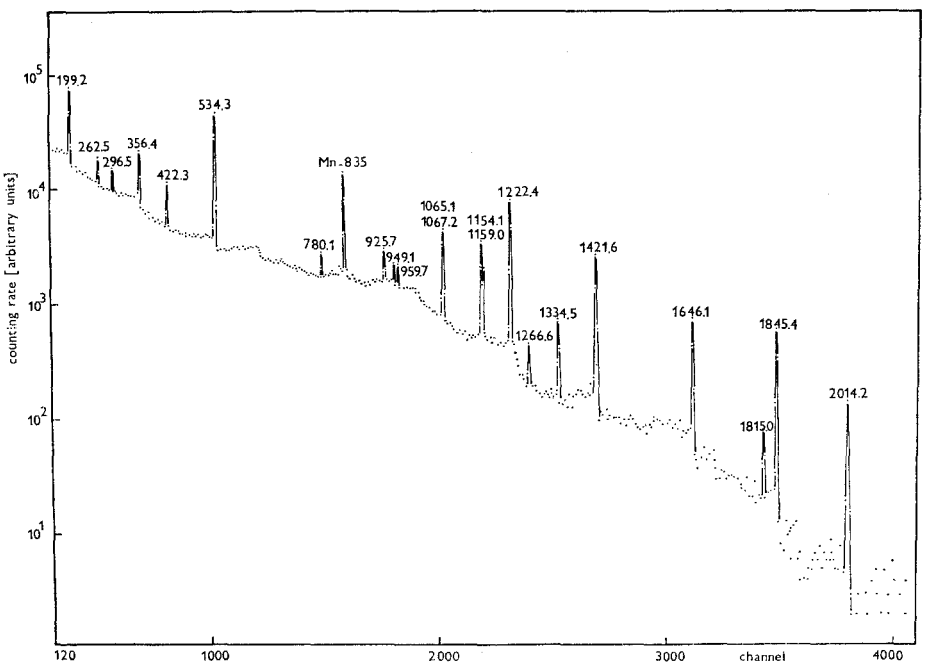

Fig. 1. Gamma-ray spectrum of ^{156}Tb taken with 30 cc Ge(Li) detector. Transition energies are given in keV.

The temperature dependence of normalized intensities $W^{exp}(\vartheta, T)$ for three transitions is shown in Fig. 2. Standard deviation in both normalized intensity and temperature is shown on measured points by bars.

Table 1

Normalized intensities of gamma-ray transitions from the decay of ^{156}Tb.

	Present work		Uluer et al. [2]	
E_γ [keV] [a]	$W^{exp}(0, T)$	$W^{exp}(\pi/2, T)$	$W^{exp}(0, T)$	$W^{exp}(\pi/2, T)$
199·2	0·789 (5)	1·091 (6)	0·800 (2)	1·105 (3)
262·5	0·851 (17)	1·116 (29)	0·872 (3)	1·093 (7)
296·5	0·759 (21)	1·111 (37)	0·749 (3)	1·132 (8)
356·4	0·669 (7)	1·131 (14)	0·682 (3)	1·150 (4)
422·3	1·143 (16)	0·914 (20)	1·137 (3)	0·946 (5)
534·3	0·627 (4)	1·201 (5)	0·637 (2)	1·188 (3)
780·1	1·237 (71)	0·938 (83)	1·254 (7)	0·875 (16)
925·7	0·920 (40)	1·042 (61)	0·899 (4)	1·061 (12)
949·1	1·398 (121)	0·914 (133)	1·261 (13)	0·936 (31)
959·7	1·109 (89)	0·942 (116)	1·076 (11)	0·963 (26)
1154·1	0·648 (12)	1·166 (29)	0·691 (3)	1·129 (5)
1159·0	1·060 (22)	0·988 (33)	1·013 (3)	0·980 (8)
1222·4	1·274 (9)	0·872 (9)	1·258 (2)	0·862 (3)
1266·6	0·699 (51)	1·046 (115)	—	—
1334·5	1·413 (44)	0·804 (42)	1·430 (5)	0·857 (10)
1421·6	0·702 (10)	1·164 (19)	0·681 (3)	1·148 (5)
1646·1	1·118 (29)	0·972 (35)	1·105 (3)	0·959 (9)
1815·0	1·068 (112)	0·938 (184)	—	—
1845·4	1·220 (28)	0·869 (29)	1·261 (3)	0·878 (8)
2014·2	1·254 (54)	0·863 (57)	1·240 (7)	0·872 (15)

[a] Gamma-ray energies taken from [18].

4. DATA ANALYSIS

4.1. Parameters of magnetic dipole and electric quadrupole hyperfine interaction

In a ^{156}Tb(Gd) sample, cooled to a low temperature in an external magnetic field $\boldsymbol{B}_{ext}$, two types of hyperfine interaction take place. They are (i) the interaction of the nuclear magnetic dipole moment μ with some effective magnetic field $\boldsymbol{B}_{eff}$, occurring in the ferromagnetic Tb–Gd solid solution [8, 9], and (ii) the interaction of the nuclear quadrupole moment Q with the finite electric field gradient which arises in hexagonal gadolinium crystals [10, 11]. If the effective magnetic field $\boldsymbol{B}_{eff}$ is parallel to the z-axis defined by the direction of the external magnetic field $\boldsymbol{B}_{ext}$ and, at the same time, the electric field gradient tensor is axially symmetric about the z-axis, the nuclear energy splitting which arises due to both the interactions can

be written in the form

$$\Delta \equiv |E_m - E_{m-1}| = \left| \frac{\mu}{I} B_{\text{eff}} - (2m - 1) P \right|, \tag{4.1}$$

where m ($\doteq -I, \ldots, +I$) is the nuclear spin component in the z-axis direction and

$$\boldsymbol{B}_{\text{eff}} = B_{\text{hf}} \boldsymbol{M}_0 + (\boldsymbol{B}_{\text{ext}} - D\boldsymbol{M}), \tag{4.2}$$

where B_{hf} is an effective value of the hyperfine field including the Lorentz field in the absence of the external field $\boldsymbol{B}_{\text{ext}}$, $\boldsymbol{M}_0$ is a unique vector in the direction of a spontaneous magnetization of a ferromagnetic domain, D is the sample demagnetization factor, $\boldsymbol{M}$ is the total magnetic moment of a sample and $D\boldsymbol{M}$ represents a demagnetizing field. The parameter P in the expression (4.1) is given for a single crystal by the relationship

$$P = P_{\parallel} + P_{\text{c}} = \frac{3eQV_{zz}}{4I(2I + 1)} + P_{\text{c}}, \tag{4.3}$$

where $V_{zz} = (\partial^2 V/\partial z^2)$ is a component of the electric field gradient tensor. $P_{\parallel}$ is a contribution of the electric field gradient at the nucleus site due to $4f$ electrons, P_{c} is a contribution of the lattice crystal field which is in metal further modified by a local non-spherically symmetrical distribution of the conduction electrons.

Parameters $X = (\mu/I) B_{\text{eff}}$ and P of the energy splitting Δ (4.1) can be extracted from the measured angular and temperature dependence of the normalized intensities $W^{\text{exp}}(\vartheta, T)$ (see Sec. 3) analyzed according to the theoretical relationship [12]

$$\begin{aligned} W(\vartheta, T) = {} & (1 - 3\varepsilon) B_2(T) A_2 U_2 Q_2 P_2(\cos\vartheta) + \\ & + (1 - 10\varepsilon) B_4(T) A_4 U_4 Q_4 P_4(\cos\vartheta). \end{aligned} \tag{4.4}$$

Here B_k are the orientation parameters which depend on the hyperfine energy splitting Δ, A_k are the angular distribution parameters depending on the gamma-ray multipole mixing ratio, U_k are the deorientation coefficients which correct for effects of unobserved intermediate radiations, Q_k are the solid-angle correction factors which account for the finite detector angular resolution and P_k are the normalized Legendre polynomials. $\varepsilon = 1 - M/M_{\text{s}}$ (M is the actual magnetization in the direction of the external field and M_{s} is the saturation magnetization) is the fractional deviation from the full magnetic saturation of a measured sample. We use formula (4.4) instead of the usual one (see e.g. [13]), since it is well known that even a small deviation from full saturation can reduce the anisotropy of radiation emitted from an oriented ensemble appreciably and our Gd matrices might not be fully saturated, although some data exist [14–16] showing that a polycrystalline Gd matrix should be saturated in an external field of about 1 T.

The extraction of values of the unknown parameters X and P by means of fitting function (4.4) to experimental data can be done in different ways. We have found

that the resulting values of the parameters may be seriously influenced by the fitting method chosen. Therefore we shall discuss the fitting problem in greater detail in the Appendix.

Parameters X and P in the present work were deduced as a weighted average of the values for the 534·3 keV line, gained by the method $B^{(b)}$ $(\vartheta=0)$ and the method D (see Appendix and Tab. 7). Values

$$X^{156} = (9{\cdot}7 \pm 1{\cdot}6) \times 10^{-25}\,\mathrm{J} \quad \text{and} \quad P^{156} = (10{\cdot}2 \pm 3{\cdot}8) \times 10^{-26}\,\mathrm{J}$$

were obtained. This result was confirmed by the analysis of some other gamma-ray transitions (199·2 keV, 1222·4 keV). The best fit of calculated to experimental values is shown in Fig. 2 by the solid curves.

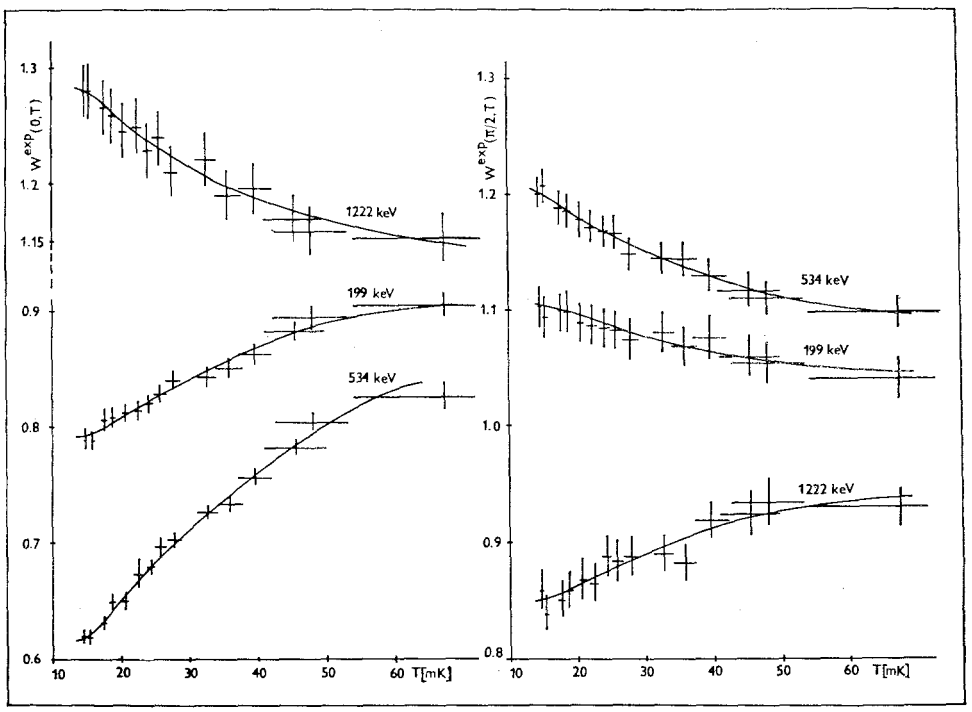

Fig. 2. Temperature dependence of $W^{exp}(\vartheta, T)$ for some transitions in ^{156}Gd.

4.2. Gamma-ray multipole mixing ratios in ^{156}Gd

Gamma-ray mixing ratios are appreciably sensible to the structure of the initial and final states of the gamma-ray transitions and can serve as sensitive test of nuclear model predictions.

If the normalized intensities of some transition at a certain temperature T and at the two angles of 0 and $\pi/2$ with respect to the applied field direction are known, it is possible to determine unambiguously values of the $k = 2$ and $k = 4$ terms in expression (4.4).

Putting

$$P(T) = (1 - 3\varepsilon)\, B_2(T)\, U_2 A_2 \tag{4.5}$$

$$S(T) = (1 - 10\varepsilon)\, B_4(T)\, U_4 A_4$$

and using the numerical values of $P_k(\cos\vartheta)$ for angles of 0 and $\pi/2$ we get

$$P^{\exp}(T) = -\frac{8[W^{\exp}(\pi/2, T) - 1] + 3\dfrac{Q_4(\pi/2)}{Q_4(0)}[1 - W^{\exp}(0, T)]}{4Q_2(\pi/2) + 3Q_4(\pi/2)\dfrac{Q_2(0)}{Q_4(0)}} \tag{4.6}$$

$$S^{\exp}(T) = -\frac{1 - W^{\exp}(0, T) + Q_2(0)\, P^{\exp}(T)}{Q_4(0)}$$

where $Q_k(\vartheta)$ are the solid-angle correction factors for detection of gamma-rays at the angle ϑ.

Using expressions (4.5) and (4.6) the angular distribution parameter A_2 may be determined whenever the values of the coefficients $B_2^{\exp} = (1 - 3\varepsilon)\, B_2(T)$, U_2 and $Q_k(\vartheta)$ are known. The parameter A_2 depends on the mixing ratio δ, i.e.

$$A_2 = \frac{F_2(L, L, I_i, I_f) + 2\delta\, F_2(L, L+1, I_i, I_f) + \delta^2\, F_2(L+1, L+1, I_i, I_f)}{1 + \delta^2} \tag{4.7}$$

where F_2 are coefficients defined and tabulated by KRANE [17] and I_i and I_f are spins of the initial and final nuclear states involved in the gamma-transition with the L and $L+1$ multipolarity components. The mixing ratio δ used in formula (4.7) is defined by means of emission matrix elements according to the phase convention of KRANE [17].

The A_4 parameter can be determined in a similar way. Due to great experimental errors this parameter is usually not suitable for determination of δ. Sometimes the sign of δ may be deduced from the experimental A_4.

In the present work the anisotropy of the 534·3 keV transition was used to derive the value of $B_2^{\exp}$, assuming the mixing ratio $\delta = 0{\cdot}06(2)$ [2] and the β-decay to the 2044·8 keV level to be the allowed Gamow-Teller type. This yields $B_2^{\exp} = 0{\cdot}914(16)$ which is used to analyse all other gamma-ray transitions.

All the nuclear spectroscopic data necessary for the calculation of the U_k coefficients were taken from the papers of FUJIOKA [18] and MCMILLAN and HAMILTON [19]. All beta-transitions, following the decay of the ^{156}Tb ground state ($I^\pi = 3^-$), were

Table 2

$E2/M1$, $M2/E1$, $M3/E2$ mixing ratios of various transitions in ^{156}Gd.

E_I [keV] (a)	U_2	U_4	E_γ [keV] (a)	$I_i^\pi \to I_f^\pi$	Mixing ratio δ (b)		
					Present work $M2/E1$	ULUER at al. [2] $M2/E1$	Other authors $M2/E1$
2103·2	0·750	0·167	2014·2	$3^- \to 2_g^+$	— 0·024 (54)	—0·013 (7)	—
			1815·0	$3^- \to 4_g^+$	0·002 (104)	—	—
			949·1	$3^- \to 2_\gamma^+$	— 0·027 (31)	— 0·025 (12)	—
2044·8	0·905	0·681	543·3	$4^- \to 4_4^+$	0·06 (2)(c)	0·06 (2)	$0{\cdot}03\ {}^{+0\cdot13}_{-0\cdot15}$ (d)
			422·3	$4^- \to 5_4^+$	0·024 (19)	— 0·009 (4)	—
1934·2	0·750	0·167	1845·4	$3^- \to 2_g^+$	— 0·008 (25)	— 0·030 (5)	$-0{\cdot}024\ {}^{+0\cdot134}_{-0\cdot126}$ (d)
			1646·1	$3^- \to 4_g^+$	— 0·015 (35)	0·012 (4)	$-0{\cdot}002\ {}^{+0\cdot063}_{-0\cdot078}$ (d)
			780·1	$3^- \to 2_\gamma^+$	0·048 (21)	— 0·024 (8)	—
					$E2/M1$	$E2/M1$	$E2/M1$
1622·4	0·850 (4)	0·543 (5)	1334·5	$5_4^+ \to 4_g^+$	$-3{\cdot}40\ {}^{+0\cdot45}_{-0\cdot57}$	— 3·8 (2)	—
			1037·9	$5_4^+ \to 6_g^+$	—	$-6{\cdot}7\ {}^{+3\cdot0}_{-21\cdot0}$	—
			115·6	$5_4^+ \to 5_\gamma^+$	—	—	$\lvert 0{\cdot}047\rvert$ (e)
			111·9	$5_4^+ \to 4_4^+$	—	$0{\cdot}15\ {}^{+0\cdot10}_{-0\cdot09}$	$\lvert 0{\cdot}089\rvert$ (e)
1510·5	0·776 (7)	0·363 (18)	1421·6	$4_4^+ \to 2_g^+$	0·002 (26)(f)	0·014 (12)(f)	—
			1222·4	$4_4^+ \to 4_g^+$	$-1{\cdot}7\ {}^{+0\cdot16}_{-0\cdot21}$	— 2·07 (13)	$-2{\cdot}12\ {}^{+0\cdot37}_{-0\cdot41}$ (d)
			925·7	$4_4^+ \to 6_g^+$	0·095 (85)(f)	0·068 (6)(f)	—
			356·4	$4_4^+ \to 2_\gamma^+$	— 0·029 (23)(f)	0·014 (12)(f)	—
			262·5	$4_4^+ \to 3_\gamma^+$	$7{\cdot}65\ {}^{+0\cdot59}_{-0\cdot51}$	$9{\cdot}2\ {}^{+0\cdot7}_{-0\cdot6}$	—
			155·2	$4_4^+ \to 4_\gamma^+$	—	—	$\lvert 0{\cdot}230\rvert$ (e)
1355·3	0·643 (18)	0·153 (53)	1266·6	$4_\gamma^+ \to 2_g^+$	$-0{\cdot}12\ {}^{+0\cdot22}_{-0\cdot28}$ (f)	—	—
			1067·2	$4_\gamma^+ \to 4_g^+$	—	$-4{\cdot}0\ {}^{+0\cdot9}_{-1\cdot6}$	—
1247·9	0·535 (17)	0·018 (7)	1159·0	$3_\gamma^+ \to 2_g^+$	$-8{\cdot}6\ {}^{+2\cdot3}_{-4\cdot8}$	$-11{\cdot}8\ {}^{+0\cdot6}_{-0\cdot7}$	$-8{\cdot}5\ {}^{+4\cdot1}_{-61\cdot6}$ (d)
			959·7	$3_\gamma^+ \to 4_g^+$	—19·3 (190)	$-11{\cdot}7\ {}^{+2\cdot7}_{-5\cdot3}$	$0{\cdot}26 \leqq \delta < 7{\cdot}44$ (d)
1154·1	0·638 (6)	0·161 (7)	1065·1	$2_\gamma^+ \to 2_g^+$	—	$-6{\cdot}5\ {}^{+2\cdot6}_{-7\cdot9}$	—

(a) Level and gamma-ray transition energies taken from [18].
(b) An error in parentheses is given in units of the last decimal.
(c) ULUER et al. [2].
(d) KENEALY et al. [29].
(e) FUJIOKA [18].
(f) $M3/E2$ mixing ratio.

assumed to be the allowed Gamow-Teller type except those to the 1622·4 keV ($I^\pi = 5^+$) and 584·7 keV ($I^\pi = 6^+$) levels, when transitions with $\Delta L > 1$ had to be considered.

The solid angle factors used in our calculations were $Q_2(0) = 0{\cdot}986$, $Q_2(\pi/2) = 0{\cdot}987$, $Q_4(0) = 0{\cdot}954$ and $Q_4(\pi/2) = 0{\cdot}957$. They have an accuracy better than 1% for all gamma-ray energies.

The mixing ratios δ for 16 gamma-ray transitions in ^{156}Gd are summarized in Tab. 2, including also results of other authors for comparison.

5. DISCUSSION

5.1. Magnetic dipole and electric quadrupole moments of ^{156}Tb

Based on the known value of the X parameter, we have deduced the nuclear magnetic dipole moment of the ^{156}Tb ground state

$$|\mu^{156}| = (9{\cdot}6 \pm 1{\cdot}3) \times 10^{-27}\ \mathrm{J/T}\,.$$

Table 3

Values of the hyperfine parameters X and P of Tb ions in the pure metal and in a dilute alloy with gadolinium.

Isotope Matrix	X [MHz]	P [MHz]	$\frac{eV_{zz}}{B_{\mathrm{eff}}}$ [(a)] $[10^{-3}$ A]	Ref.
^{159}Tb in pure metal	3120	337	8·49	Sano et al. in Ref. [11]
~10% ^{159}Tb ~90% Gd dilute alloy	3068	351	8·99	Kobayshi [10]
^{156}Tb ~100% Gd dilute alloy	1460	154	8·99 [(b)]	present work
^{156}Tb ~100% Gd dilute alloy	1460	154	14·4	X, P - present μ^{156}, Q^{156} from Ref. [1]

(a) $\frac{eV_{zz}}{B_{\mathrm{eff}}} = \frac{4}{3}(2I-1)\frac{P}{X}\frac{\mu}{Q}$.

(b) Values V_{zz} and B_{eff} in the present work are taken from [10].

The value of the effective magnetic field $B_{\mathrm{eff}} \doteq B_{\mathrm{hf}} \doteq 303(3)$ T was taken from [10]. The term $B_{\mathrm{ext}} - DM$ in eq. (4.2) has the value of 0·7 T and can be neglected. The hyperfine magnetic field B_{hf} measured in [10] for a dilute alloy of about 10% ^{159}Tb, 90% Gd can be used for a solid solution of a trace amount of ^{156}Tb in Gd under the assumption that the hyperfine magnetic field for a Tb–Gd solid solution is independent on both the terbium isotope mass number (i.e. hyperfine magnetic anomaly is small) and the concentration of Tb atoms in gadolinium. Actually, from the experimental results summarized by BLEANY [11] it follows that the magnetic hyperfine anomaly is very weak for rare earths. The dependence of the Tb–Gd hyperfine magnetic field on a concentration of Tb atoms is illustrated in Tab. 3, taken from [11] and supplemented by our results. From the comparison of X values for different concentration of ^{159}Tb atoms it follows that the ~90% change of the concentration causes only a ~2% change of the parameter X. The result enables us to suppose the concentration dependence of Tb–Gd hyperfine magnetic field not to be significant.

Assuming the magnetic hyperfine anomaly to be negligible, it is to expect that the ratio of magnetic hyperfine splittings for different pairs of Tb isotopes in gadolinium should have the same value as the corresponding ratio of gyromagnetic factors, i.e.

$$\frac{X^I}{X^{II}} \doteq \frac{(\mu/I)^I}{(\mu/I)^{II}} \doteq \frac{g^I}{g^{II}}.$$

Using for such a comparison the ^{160}Tb isotope, for which the magnetic moment [20] and the magnetic hyperfine splitting [21, 22] are known, we get $X^{160}/X^{156} = 0{\cdot}9 \pm \pm 0{\cdot}2$. The gyromagnetic ratio for our value of μ^{156} is $0{\cdot}89 \pm 0{\cdot}14$, which is in very good agreement with the X parameters ratio, while for the value of μ^{156}, reported in [1], we obtain $g^{160}/g^{156} = 1{\cdot}16 \pm 0{\cdot}13$. Further, using the value of μ^{156} from [1] and the present value of X^{156}, we deduce $B_{\mathrm{hf}} = (400 \pm 70)$ T, which disagrees with the value of KOBYASHI [10]. The discrepancies shown above can hardly be explained by a magnetic hyperfine anomaly and therefore we suppose them demonstrating the preference of our value of μ^{156} over that from the work [1].

Another way of verification of our results follows from the systematics of magnetic dipole moments of the ground states of odd-odd Tb isotopes. It is well known [23] that the ground states of that the ground states of $^{156,158\text{ and }160}$Tb have the same single-particle structure p 411↑ + n 521↑ with intrinsic spins parallel. Neglecting residual interaction between the odd nucleons, the ground states of these Tb isotopes are expected to have the same magnetic dipole moment. The assumption is valid for ^{158}Tb [24] and ^{160}Tb [20] within the experimental errors, but the result [1] for ^{156}Tb is slightly lower. Theoretical calculations, using the detailed Nilsson wave functions ($\eta = +6$) and neglecting the odd-particle correlations, give the value $\mu = +10.1 \times 10^{-27}$ J/T [25]. Using the experimental values of μ for the ^{159}Tb ground state (411↑) [24] and the average value of μ for the ^{155}Gd and ^{157}Dy ground

states (521↑) [26], we obtain $\mu = +8{\cdot}64 \times 10^{-27}$ J/T, neglecting again the correlations between the odd proton and neutron and assuming a parallel orientation of their spins.

Our result is in quite good agreement with both presented theoretical and experimental estimates. We note that according to theoretical calculations and systematics of magnetic moments of odd-odd nuclei the positive sign of μ^{156} is expected.

To deduce the electric quadrupole moment Q^{156} from the experimental value of the parameter P, it is necessary to discuss the physical interpretation of the parameter for the case of ^{156}Tb ions dissolved in a polycrystalline Gd matrix. If we apply an external magnetic field to such a sample and the sample reaches the state of full magnetic saturation, then the $4f$ electrons magnetization is parallel to the direction of the applied field (z-axis), but the direction of the hexagonal axis c of a microcrystal of the matrix forms a random angle ξ with the z-axis. Since in a metallic lattice the electric field gradient has the symmetry of the lattice, the resulting electric field gradient tensor is no longer axially symmetric about the z-axis in a polycrystalline Gd matrix. In such a case we have to rewrite expression (4.3) for an individual crystal to the form [11]

$$P = P_{\parallel} + \tfrac{1}{2}(3\cos^2\xi - 1)\,P_c\,.$$

For a polycrystalline matrix including many randomly oriented microcrystals, it is possible to consider the quantity P as an average value over all orientations of the microcrystals in space. Recently HAROUTUNIAN and MEYER [27] have calculated exactly the general expression for the angular distribution of radiation emitted by an oriented state for polycrystalline samples, where the principal axes of the electric field gradients are randomly distributed with respect to a fixed magnetic field direction. They have shown that unless the quadrupole splitting is of the same order of magnitude as the magnetic one, but smaller, expression (4.3) is acceptable for polycrystalline samples. Further, for the majority of rare earths, including Tb [11], the numerical value of P_c is only 5–10% of the value of $P_{\parallel}$. Therefore we assume $P^{156} = P_{\parallel}$. Deducing the V_{zz} value for Tb–Gd on the basis of the known values of the quadrupole electric moment Q [24] and the parameter P [10] for ^{159}Tb, we get

$$Q^{156} = (2{\cdot}9 \pm 0{\cdot}9) \times 10^{-28}\ \mathrm{m}^2\,.$$

The result, in spite of the considerable experimental error, seems to be more plausible than the value of Q^{156} reported in [1].

To prove it, we can use the known values of Q^{160} [20] and P^{160} [21, 22]. Within the limit of experimental errors and the error due to the negligence of the contribution P_c it should be

$$\frac{P^{160}}{P^{156}} \doteq \frac{Q^{160}}{Q^{156}}\,.$$

Using P^{156} from the present work and the weighted average of the values of P^{160}

from the works [21] and [22] we have

$$\frac{P^{160}}{P^{156}} = 1{\cdot}1 \pm 0{\cdot}5 \quad \text{and} \quad \frac{Q^{160}}{Q^{156}} = 1{\cdot}1 \pm 0{\cdot}4\,,$$

where Q^{160} is taken from the paper [20] and Q^{156} is the present value. The ratio of quadrupole moments for the old value of Q^{156} [1] is $2{\cdot}1 \pm 0{\cdot}8$, which differs from the ratio of corresponding quadrupole splittings. As can be seen in Tab. 3, not even the quantity eV_{zz}/B_{eff}, calculated for the values of μ^{156} and Q^{156} from the work [1] agrees with the other ones. The deviation can be explained neither by the dependence of this quantity on the Tb isotope mass number, nor by the different concentration of Tb atoms in gadolinium, because it can be easily shown that the ratio eV_{zz}/B_{eff} is determined only by an electronic structure in a Tb–Gd alloy.

On the basis of our results it is possible to estimate the value of the intrinsic quadrupole moment of the ^{156}Tb nucleus. We get $Q_0^{156} = (6{\cdot}9 \pm 1{\cdot}4) \times 10^{-28}$ m^2, which is in good agreement with the known values of Q_0 for neighbouring Tb nuclei: $Q_0^{158} = (6{\cdot}5 \pm 1{\cdot}2) \times 10^{-28}$ m^2 and $Q_0^{160} = (7{\cdot}2 \pm 1{\cdot}2) \times 10^{-28}$ m^2 [28].

5.2. Multipole mixing ratios of transitions in ^{156}Gd

The ^{156}Gd nucleus is situated at the onset of the deformed region and many of its excited states have collective features. Nevertheless, some of their characteristics are not understood in terms of phenomenological collective models. HAMILTON et al. [30] have studied the multipole mixing ratio of the transition $2_\beta^+ \to 2_g^+$ to find such a $M1$ admixture which might account for the discrepancy between theoretical [31] and experimental values of $B(E2)$ branching ratios for transitions from the beta-vibrational band to the ground state band. It has been shown that such an admixture does not exist, as in ^{152}Sm [32] and ^{154}Gd [33].

Systematic investigation of $B(E1)$ and $B(E2)$ branching ratios for transitions in ^{156}Gd has been performed by many authors (see e.g. [18, 19, 34]). Calculations of the reduced probability ratios have been mostly realized under the assumption that the transitions involved have the pure $E1$ or $E2$ multipolarity and the results obtained have been compared to theoretical values calculated in terms of a rotational-vibrational model [35] and a pairing-plus-quadrupole model [3]. In some cases the comparison shows satisfactory agreement but sometimes considerable disagreement is observed. ULUER et al. [2] have determined the multipole character of twenty-one transitions in ^{156}Gd. Our results confirm within the limits of experimental errors almost all the results of the work [2].

As can be seen in Tab. 4, the $M1$ (or $M3$) admixtures found in the transitions from the gamma-vibrational and $K^\pi = 4^+$ bands cannot change essentially the discrepancy between the theoretical and experimental values of the $B(E2)$ branching ratios, as in the case of the beta-vibrational band [30].

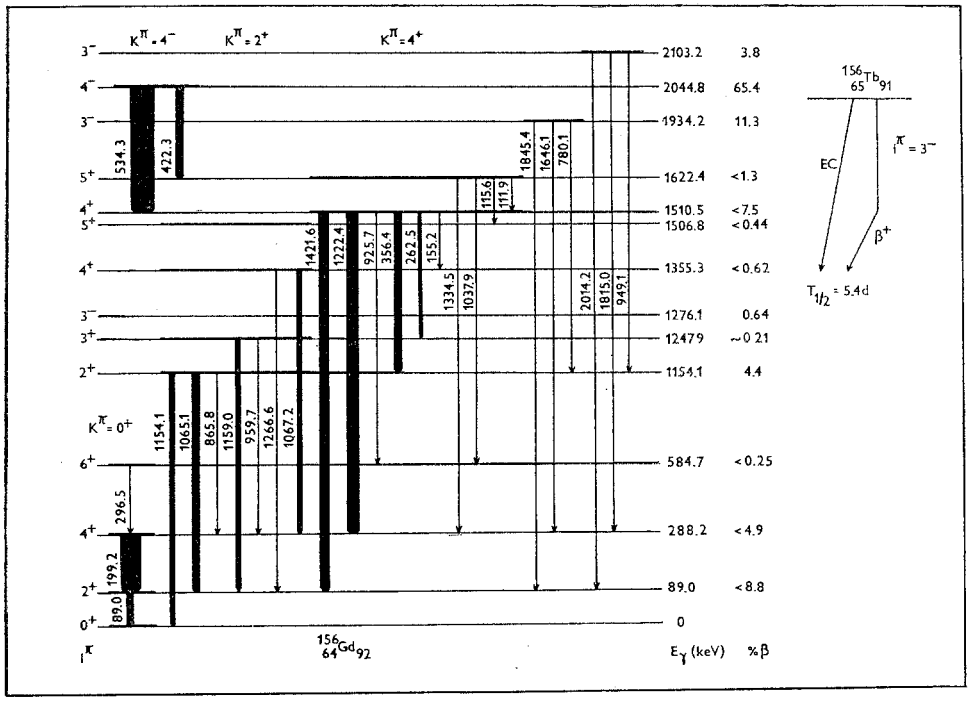

Fig. 3. A fragment of the scheme of excited levels in ^{156}Gd, populated following the β^+ and EC decay of ^{156}Tb ($T_{1/2} = 5{\cdot}4$ d).

The present work confirms also the existence of a large $M1$ admixture into the 1222·4 keV $4_4^+ \rightarrow 4_g^+$ transition which has been reported previously by several authors [2, 18, 19, 36]. The admixture supports the interpretation of the 1510·5 keV $K^\pi I = 4^+4$ level as a proton two-quasiparticle state p 413↑ + p 411↑, $\Sigma = 0$ [37], with a small collective admixture. Really, FUJIOKA [18] has estimated the beta- and gamma-vibrational bands admixtures into the 1510·5 keV state and he has found them to be very small. The same conclusion has been made by GRIGORJEV and SOLOVIEV [38] on the basis of an analysis of $B(E1)$ values for the $E1$ transitions from the 2044·8 keV proton two-quasiparticle state p 532↑ + p 411↑, $\Sigma = 1$ ($K^\pi I = 4^-4$) to the gamma-vibrational and $K^\pi = 4^+$ bands. The $B(E1)$ values for transitions to the 4^+ and 5^+ states of the gamma-vibrational band are of 2−3 orders of magnitude lower than for transitions to the 4^+ and 5^+ states of the $K^\pi = 4^+$ band. This fact gives evidence for a slight mixing of states with $\Delta K = 2$.

Assuming the half-life of the 1510·5 keV state to be $T_{1/2} = (0{\cdot}188 \pm 0{\cdot}010)$ ns [39], it is possible to calculate the experimental values of reduced transition probabilities for $M1$ and $E2$ components of the $4_4^+ \rightarrow 4_g^+$ 1222·4 keV transition. This yields $B(M1) = (3{\cdot}4 \pm 1{\cdot}0) \times 10^{-58}$ J^2/T^2 and $B(E2) = (9{\cdot}2 \pm 2{\cdot}7) \times 10^{-99}$ C^{2}m^4. The $B(E2)$ value agrees better with the theoretical one $B(E2)_{th} = 6{\cdot}7 \times 10^{-99}$ C^{2}m^4 [3] than

Table 4

$B(E2)$ branching ratios for transitions from the $K^\pi = 4^+$ and and gamma-vibrational bands in ^{156}Gd.

I_i	I_f/I_f'	E_γ [keV]	$B(E2)$ ratio			
			Theor.[a]	Theor.[b]	Exp. (present)[c]	Exp.[d]
4_4	$2_g/4_g$	1422/1222	1·3	0·34	0·25 (5)	0·23 (1)
	$6_g/2_g$	926/1422	—	0·25	2·71 (44)	2·72 (14)
	$6_g/4_g$	926/1222	—	0·09	0·67 (6)	0·62 (2)
	$3_\gamma/2_\gamma$	263/357	1·13	0·56	2·00 (25)	2·03 (13)
	$4_\gamma/2_\gamma$	155/357	0·41	—	1·47 (30)	1·46 (25)
	$4_\gamma/3_\gamma$	155/263	0·36	—	0·73 (25)	0·71 (14)
2_γ	$0_g/2_g$	1154/1065	0·64	—	0·67 (9)	0·67 (3)[e]
	$4_g/2_g$	866/1065	0·20	—	0·084 (24)	0·086 (17)[e]
3_γ	$2_g/4_g$	1159/960	1·38	—	1·50 (12)	1·52 (8)[e]
4_γ	$2_g/4_g$	1266/1067	0·40	—	0·159 (48)	0·152 (13)[f]

[a] Pairing-plus-quadrupole model [3].

[b] Rotation-vibration model [35].

[c] $B(E2)$ ratios calculated including the mixing ratios in Tab. 2. Gamma-ray transition intensities were taken from Ref. [19], the 155 keV transition was taken to be 18·7% $E2$.

[d] Values from Ref. [19], where the 155 and 1222 keV transitions were taken to be 18·7% $E2$ and 81% $E2$, respectively. All the other transitions were supposed to have a pure multipolarity.

[e] KLUK et al. [34].

[f] MCMILLAN et al. [19].

Table 5

Theoretical and experimental $E2/M1$ mixing ratios for transitions from the gamma-vibration band in ^{156}Gd.

$I_i \to I_f$	E_γ [keV]	$\delta^{\text{theor (a)}}$	δ^{exp}
$2_\gamma \to 2_g$	1065	—41·0	$-6{\cdot}5\ ^{+2{\cdot}6\,[b]}_{-7{\cdot}9}$
$3_\gamma \to 2_g$	1159	—57·5	$-8{\cdot}6\ ^{+2{\cdot}3}_{-4{\cdot}8}$
$3_\gamma \to 4_g$	960	—37·3	$-19{\cdot}3 \pm 19$
$4_\gamma \to 4_g$	1067	13·7	$-4{\cdot}0\ ^{+0{\cdot}9\,[b]}_{-1{\cdot}6}$

[a] Pairing-plus-quadrupole model [3].

[b] ULUER et al. [2].

the value $B(E2) = 12{\cdot}3 \times 10^{-99}$ C^{2}m^4 [40] deduced on the assumption that the 1222·4 keV transition has pure $E2$ multipolarity. Unfortunately, similar comparison for the $M1$ component is impossible because the theoretical $B(M1)$ value has not been calculated.

The negative parity 1934·2 (3^-), 2044·8(4^-) and 2103·2 keV (3^-) levels are deexcited via $E1$ transitions with $M2$ admixtures less than 0·4%. It is interesting that the mixing ratios of $E1$ transitions from the 1934·2 and 2103·2 keV levels to the ground state band have the same sign (except for the weak 1815·0 keV transition whose δ has a large experimental error). This may be in connection with the predicted same two-quasiparticle structure of the states [38].

A comparison of our results and the results of the work [2] to the theoretical values of δ [3] for transitions from the gamma-vibrational to the ground state band is shown in Tab. 5. It can be seen that in all cases the theory gives larger values of δ than are the experimental ones and for the $4^+_\gamma \rightarrow 4^+_g$ transition moreover an opposite sign of the mixing ratio.

6. CONCLUSIONS

Parameters of hyperfine magnetic dipole and electric quadrupole interactions in ^{156}Tb – Gd solid solution and corresponding magnetic dipole and electric quadrupole moments of the ^{156}Tb ground state have been found. All the values mentioned are in good agreement with the systematics of existing experimental and theoretical data. It has been shown that the parameter P of the electric quadrupole interaction in Tb – Gd solid solution is determined predominantly by the electric field gradient at the nucleus site due to $4f$ electrons and therefore the expression for P, holding for an individual crystal, can also be used for a polycrystalline matrix.

From the present analysis of multipole mixing ratios of transitions in ^{156}Gd it has followed that $M1$ (or $M3$) admixtures, found in the transitions deexciting the gamma-vibrational and $K^\pi = 4^+$ bands, cannot change essentially the discrepancy between the theoretical and experimental values of the $B(E2)$ branching ratios. The multipole mixing ratios of the 1222·4 keV transition and of the transitions from the negative parity states seem to confirm theoretical interpretation of the initial states of these transitions.

APPENDIX

To calculate the values of the parameters X and P by fitting the theoretical function (4.4) to experimental data, it is convenient to rewrite expression (4.4) to the form

$$W(X, P, \vartheta, T) = 1 + K_2(\vartheta)\, B_2(X, P, T) + K_4(\vartheta)\, B_4(X, P, T)\,, \tag{A.1}$$

where

$$K_2(\vartheta) = (1 - 3\varepsilon)\, A_2 U_2 Q_2 P_2(\cos\vartheta) \quad \text{and}$$

$$K_4(\vartheta) = (1 - 10\varepsilon)\, A_4 U_4 Q_4 P_4(\cos\vartheta)\,.$$

The choice of a suitable fitting procedure depends predominantly on the conditions of the experiment and on our knowledge of various parameters of the fitted function. In the next we shall discuss four possible treatments of the problem.

A) A method frequently used [1, 25, 41] is to fix the parameters $K_2(\vartheta)$ and $K_4(\vartheta)$ in eq. (A.1) which are supposed to be known and to reduce the problem to searching for the parameters X and P by minimization of the functional

$$\chi^2(X, P) = \sum_{i=1}^{N} w_i[W^{\exp}(\vartheta, T_i) - W(X, P, \vartheta, T_i)]^2 \tag{A.2}$$

for a given angle ϑ. Here $W^{\exp}(\vartheta, T_i)$ is the normalized intensity of a gamma-ray transition measured at a temperature T_i (values T_i are assumed to be known and their experimental errors are not included into the calculation), the function W is given by relationship (A.1), w_i is the statistical weight of the i^{th} experimental point and N is the number of all experimental points.

B) Four parameters X, P, $K_2(\vartheta)$ and $K_4(\vartheta)$ are calculated by means of minimization of the functional

$$\chi^2(X, P, K_2, K_4) = \sum_{i=1}^{N} w_i[W^{\exp}(\vartheta, T_i) - W(X, P, K_2, K_4, \vartheta, T_i)]^2 \tag{A.3}$$

for a given angle ϑ. All quantities appearing in expression (A.3) have the same meaning as in equation (A.2).

C) Including experimental errors of the values T_i into the calculation B, the form of the minimized functional becomes

$$\chi^2(X, P, K_2, K_4, T_i, W_i, \lambda_i) = \tag{A.4}$$
$$= \sum_{i=1}^{N} [w_{T_i}(T_i^{\exp} - T_i)^2 + w_i(W^{\exp}(\vartheta, T_i) - W_i)^2 + 2\lambda_i F(X, P, K_2, K_4, \vartheta, T_i, W_i)],$$

where w_{T_i} and w_i are statistical weights of T_i and $W^{\exp}(\vartheta, T_i)$ respectively; λ_i is a Lagrange multiplicator and the functions F represent N binding conditions of the type

$$F(X, P, K_2, K_4, \vartheta, T_i, W_i) \equiv W_i - W(X, P, K_2, K_4, \vartheta, T_i) = 0 \tag{A.5}$$

which also define the parameter W_i.

D) If the temperature dependence of the normalized intensities $W^{\exp}(\vartheta, T_i)$ is measured at least at two independent angles ϑ, it is possible to determine unambiguously experimental values $P^{\exp}(T_i)$ and $S^{\exp}(T_i)$ of the quantities $P(T)$ and $S(T)$ (see Sec. 4, eqs. (4.4) and (4.6)). It is clear that the ratios

$$R_i^{\exp} = P^{\exp}(T_i)/P^{\exp}(T_R) \quad \text{and}$$
$$Q_i^{\exp} = S^{\exp}(T_i)/S^{\exp}(T_R)$$

for two different temperatures T_i and T_R are independent on the parameters ε, U_2, U_4, A_2, A_4. Using this fact, we can write the minimized functional for a search for the parameters X and P in the form

$$\chi^2(X, P, T_i, R_i, Q_i, \lambda_i^F, \lambda_i^G) = \sum_{i=1}^{N} [w_{T_i}(T_i^{\exp} - T_i)^2 + \tag{A.6}$$
$$+ w_{R_i}(R_i^{\exp} - R_i)^2 + 2w_{R_iQ_i}(R_i^{\exp} - R_i)(Q_i^{\exp} - Q_i) +$$
$$+ 2\lambda_i^F F(X, P, T_i, R_i) + 2\lambda_i^G G(X, P, T_i, Q_i)],$$

with binding conditions

$$F(X, P, T_i, R_i) = R_i - \frac{B_2(X, P, T_i)}{B_2(X, P, T_R)} = 0 \quad \text{and} \tag{A.7}$$
$$G(X, P, T_i, Q_i) = Q_i - \frac{B_4(X, P, T_i)}{B_4(X, P, T_R)} = 0 .$$

The term $2w_{R_iQ_i}(R_i^{\exp} - R_i)(Q_i^{\exp} - Q_i)$ in equation (A.6) expresses the correlation between experimental errors of the quantities $R_i^{\exp}$ and $Q_i^{\exp}$. Parameters R_i and Q_i are defined by conditions (A.7). The temperature T_R is an arbitrary one from the set of N measured values T_i. All other quantities appearing in (A.6) have the same meaning as the analogical ones in (A.4). It should be noted that the quantities T_R, $P(T_R)$ and $S(T_R)$ are assumed to be without experimental errors.

Table 6

Results of the fitting method D for different values of T_R.

$X(\Delta X)$ [10^{-25} J]	$P(\Delta P)$ [10^{-26} J]	T_R [mK]	R^2 [a]
9·69 ± 1·55	10·4 ± 3·8	14·6	131
9·68 ± 1·51	11·7 ± 4·3	15·1	150
9·74 ± 1·77	10·9 ± 4·8	17·4	189

[a] $R^2 = \sum_{i=1}^{N} [(T_i^{\exp} - T_i)^2 + (R_i^{\exp} - R_i)^2 + (Q_i^{\exp} - Q_i)^2 +$
$+ 2(R_i^{\exp} - R_i)(Q_i^{\exp} - Q_i)]$

We shortly summarize the main advantages and difficulties of each method presented. In the case A a systematical error in calculated parameters can arise due to our poor knowledge of precise values of the parameters $K_2(\vartheta)$ and $K_4(\vartheta)$ (especially of the quantity ε). In the method B this disadvantage is excluded but, similarly to in the method A, experimental errors of temperatures are not included into the calculation. However, if the temperatures are determined using a nuclear thermometer,

the errors are greater of or the same order of magnitude as errors of $W^{exp}(T_i)$ and their absolute values vary with T_i appreciably. This difficulty is eliminated in the methods C and D. Results of the method C may be influenced by the uncertainty in the choice of the value T_R. The error can be reduced considerably if we choose the value of T_R in the region of the maximal sensitivity of the nuclear thermometer used [12]. Nevertheless, it is better to repeat the calculation for several values of T_R and to take the result leading to the lowest value of the criterion χ^2 (or R^2). As can be seen in Tab. 6, in the most cases the effect of the choice of T_R on the values of X and P is within the limits of experimental errors. The advantage of the method D is fast convergence of the fitting process and the fact that results are affected only by the two-dimensional correlation between the unknown parameters compared to the four-dimensional correlation in the cases B and C.

Table 7

Values of the parameters X and P obtained by different methods of fitting the theoretical curve (4.4) to experimental data for the 543·3 keV transition.

$X(\Delta X)$ [10^{-25} J]	$P(\Delta P)$ [10^{-26} J]	Fitting procedure	
13·6 ± 3·6	24·2 ± 4·7	A[a]	$\varepsilon = 0$; $\vartheta = 0$; $\delta = 0{\cdot}06$ (2)
10·4 ± 2·2	12·0 ± 5·3	B[a]	$\vartheta = 0$
9·69 ± 1·73	10·0 ± 3·7	B[b]	$\vartheta = 0$
10·4 ± 1·8	10·9 ± 4·6	B[b]	$\vartheta = \pi/2$
10·4 ± 1·6	9·9 ± 3·3	C[a]	$\vartheta = 0$
9·69 ± 1·55	10·4 ± 3·8	D	$\vartheta = 0, \pi/2$; $T_R = 14{\cdot}6$ mK

[a] Experimental values of temperature were taken.
[b] Corrected values of temperature were taken.

Illustrating results of the methods mentioned are summarized in Tab. 7 for the 534·3 transition. For minimization of the χ^2 functional the SIMPLEX method [42] (cases A, B) and the GAUSS-NEWTON method (cases C, D) were used. From Tab. 7 it follows that all results are in agreement within errors but the case A, where neither the absolute values of parameters X and P, nor their ratio agree with the results of the other methods. The calculation B was performed on the one hand using experimental values of temperature and on the other hand using "corrected" temperatures, calculated by means of the method D. The latter treatment yields smaller uncertainties in the X and P parameters.

The authors are indebted to I. I. Gromova for mass-separation of the measured samples, to V. M. Tsupko-Sitnikov and M. I. Fominikh for help with the arrangement of the experimental equipment and data transmission, to J. Gavor and V. Deriuga for assistance in the data processing and to Dr. M. Odehnal for reading the manuscript and valuable remarks.

Received 26. 9. 1978.

References

[1] Lovejoy C. A., Shirley D. A., Nucl. Phys. *30* (1962), 452.
[2] Uluer I., Kalfas C. A., Hamilton W. D., Fox R. A., Warner D. D., Finger M., Do Kim Chung, J. Phys. G: Nucl. Phys. *1* (1975), 476.
[3] Gupta J. B., Kumar K., Hamilton J. H., Phys. Rev. *C 16* (1977), 427.
[4] Gromova I. I., Dupak J., Konitchek J., Kracikova T. I., Lebedev N. A., Machova A., Neganov B. S., Ota J., Pavlov V. N., Prokhazka I., Rhzikovska I., Finger M., Fominikh V. I., Fominikh M. I., Shchus A. F., Chan Chen Mo, Cupko-Sitnikov V. M., Janout Z., JINR R 13-11363 (1975).
[5] Pavlov V. N., Neganov B. S., Konitchek J., Ota J., Cryogenics *18* (1978), 115.
[6] Dupak J., Konitchek J., Machova A., Pavlov V. N., Rhzikovska I., Finger M., Khadima A., Shchus A. F., Proceedings of the 27th Conference on Nuclear Spectroscopy and Structure of Atomic Nuclei, Tashkent 1977, p. 367.
[7] Osborne J. A., Phys. Rev. *67* (1945), 351.
[8] Shunk F. A., *in* Constitution of binary alloys, Second supplement, McGraw-Hill, New York 1969.
[9] Taylor K. N. R., Darby M. I., Physics of Rare Earth Compounds, Chapman and Hall, London 1972.
[10] Kobayshi S., Sano N., Itoh J., J. Phys. Soc. Japan *23* (1967), 474.
[11] Bleany B., *in* Magnetic Properties of Rare Earth Metals. (Ed. R. J. Elliot.) New York 1972.
[12] Berglund P. M., Collan H. K., Ehnholm G. J., Gylling R. G., Lounasmaa O. V., J. Low Temp. Phys. *6* (1972), 357.
[13] Hamilton W. D., *in* The Electromagnetic Interaction in Nuclear Physics. (Ed. W. D. Hamilton.) North-Holland, Amsterdam 1975.
[14] Elliot J. F., Legvold S., Spedding F. H., Phys. Bev. *91* (1953), 28.
[15] Trombe F., Ann. Phys. *7* (1937), 383.
[16] Cameron J. A., Campbell I. A., Compton J. P., Grant M. F., Hill R. W., Lines R. A., Low Temperature Physics-LT9 Part B, Plenum Press, New York 1965.
[17] Krane K. S., Report Los Alamos LA-4677 (1971).
[18] Fujioka M., Nucl. Phys. *A 153* (1970), 337.
[19] McMillan D. J., Hamilton J. H., Phys. Rev. *C 4* (1971), 542.
[20] Easly W. C., Barclay J. A., Shirley D. A., Phys. Rev. *170* (1968), 1083.
[21] Gromova I. I., Dupak J., Konitchek J., Kracikova T. I., Lebedev N. A., Neganov B. S., Pavlov V. N., Prokhazka I., Finger M., Tsupkositnikov V. M., Shchus A. F., Machova A., Hamilton W. D., Fox R. A., Preprint JINR 6-11871 (1978).
[22] Erzinkian A, L., Muravieva V. V., Parfenova V. P., Turovcev V. V., Shpinel V. C., JETP *72* (1977), 1902.
[23] Elmore D., Thesis, University of Rocherster, 1974.
[24] Avotina M. P., Zolotavin A. V., Moments of Ground and Excited States on Nuclei, Leningrad 1976.
[25] Johnson C. E., Schooley J. F., Shirley D. A., Phys. Rev. *120* (1960), 2108.
[26] Lindgren I., *in* Alpha-, Beta- and Gamma-Ray Spectroscopy. (Ed. K. Siegbahn.) North-Holland, Amsterdam 1964.
[27] Haroutunian R., Meyer M., Phys. Rev. *C 17* (1978), 292.
[28] Löbner K. E. G., Vetter M., Hönig V., Nucl. Data Tables *A 7* (1970), 495.
[29] Keanely P. F., Funk E. G., Mihelich J. W., Nucl. Phys. *A 105* (1967), 522.
[30] Hamilton J. H., Little P. E., Ramayya A. V., Collins E., Phys. Rev. *C 5* (1972), 899.
[31] Mottelson B. R., J. Phys. Soc. Japan Suppl. *24* (1968), 87.
[32] Hamilton J. H., Ramayya A. V., Whitlock L. C., Phys. Rev. Letters *22* (1969), 65.

[33] FRASER I. A., GREENBERG J. S., SIE S. H., STOKSTAND R. G., BURGINYON G. A., BROMLEY D. A., Phys. Rev. Letters *23* (1969), 1047.
[34] KLUK A. F., JOHNSON N. R., HAMILTON J. H., Z. Physik *253* (1972), 1.
[35] BOHR A., MOTTELSON B. R., Nuclear Structure, Benjamin, New York 1975.
[36] MCMILLAN D. J., HAMILTON J. H., MLADJENOVIC M., Z. Physík *241* (1971), 103.
[37] PJATOV N. I., SOLOVIEV V. G., Izv. Akad. Nauk USSR, ser fiz. *28* (1964), 11.
[38] GRIGORIEV E. P., SOLOVIEV V. G., Structure of Even-Even Deformed Nuclei, Nauka, Moskva 1974.
[39] BELL R. E., JORGENSEN M. H., Nucl. Phys. *12* (1959), 413.
[40] ANDREJTSCHEFF V., SCHILLING K. D., MANFRASS P., Atomic Data and Nucl. Data Tables *16* (1975), 515.
[41] FOX R. A., HAMILTON W. D., *in* Proc. Int. Conf. on Rare Earths, Uppsala 1974.
[42] NELDER J. A., MEAT R., The Comp. Journ. *7* (1965), 308.